IOP Conf. Series: Materials Science and Engineering **398** (2018) 012028 doi:10.1088/1757-899X/398/1/012028

A Novel Measurement for Monitoring Mechanical Impedance Applied to Breakthrough Detection of Bone-Drill System

P J Ko[1] **and M C Tsai**[1]
[1]Department of Mechanical Engineering, National Cheng Kung University, No.1, Ta-Hsueh Road, Tainan 701, Taiwan

Abstract. Based on a Chain Scattering Description and the Hilbert Huang Transform, this paper proposes a new measurement for monitoring dynamic changes of mechanical impedance without applying conventionally mechanical sensors. The proposed method is applied to the bone drilling system to detect the moment of bone breakthrough. The single frequency mechanical impedance of bone can be computed from the electrical signal of a DC motor in accordance with the proposed method. The experimental results demonstrate that the moment of bone breakthrough can accurately be detected by monitoring changes of mechanical impedance.

1. Introduction

Bone drilling is frequently performed in medical surgery, such as nail insertions for tooth implantation, orthopedic surgery, neurosurgery, maxillofacial surgery, osteosynthesis, etc. During a bone drilling procedure, a hole through the bone is created by the surgeon with a drilling machine. The surgeon determines the moment of bone breakage from his or her experience. However, bones in the human body are surrounded by blood vessels and nerves. Even the slightest deviation can damage these tissues and threaten the life of patients. Therefore, many studies have been devoted to the techniques of automatically detecting the moment of bone breakthrough since 1996 [1][2][3][4]. Allotta et al. [1] proposed a theoretical model for estimating penetration force during bone-drilling. Then, an upper limit threshold to the first derivative of the penetration force could be set according to the theoretical model, which was applied to detecting the moment of bone breakthrough. Ong and Bouazza-Marouf [2] proposed a different breakthrough detection technique. This technique converted the profiles of drilling force differences between successive samples and/or the drill bit rotational speed into easily recognizable and more consistent profiles by using a modified Kalman filter, which allows a robust and repeatable detection of breakthrough. The established breakthrough detection methodologies in most of the literature were based on the penetration force from the load cell, which suffers from sensor noise. Moreover, given the diversity of human bone density and thickness, a thrust-force signal will have many spurious pulse noises during the drilling process. Therefore, Colla and Allotta [3] presented an alternative breakthrough detection method based on wavelets. They detected bone breakthrough based on wavelet analysis of the thrust force signal. Besides, Lee et al. [4] realized an automatic bone drilling machine that can automatically stop by analyzing the thrust force, drilling torque, and feed rate velocity signals once the system breaks through bone.

Previous studies use the information of load cells or torque sensors mounted on the bone drilling machine. Unfortunately, there is usually an installation issue in the load cell and torque sensor. Moreover, a breakthrough detection technique based on a force/torque signal without using velocity information might easily lead to improper monitoring decisions due to that the bone has an inhomogeneous organic nature of variable impedance. In this paper, through the Chain Scattering Description (CSD) [5] with Hilbert Huang Transform (HHT) technology [6], the equivalent

mechanical impedance of bone is detected by measuring the electrical signal in the bone drilling machine, which means the electromechanical actuator is designed to serve as a sensor in order to avoid the installation issues associated with the force sensor. In accordance with monitoring the equivalent mechanical impedance, the evaluation and determination mechanism of breakthrough detection is established, which has the advantage of considering force and velocity information simultaneously to avoid improper monitoring decisions.

2. Experimental bone drilling system

The experimental bone drilling system is shown in figure 1. The servo feed system is a linear motor (Copley Controls Corp. TB2504), which is driven by a velocity-mode driver. The bone drilling system consists of a drill bit and a DC drilling motor. Further, a PID speed controller was designed in a DC drilling motor [7] to effectively strengthen the rigidity and expel the heat to avoid tissue damage caused by high temperatures [8] as shown in figure 2. Given the parameters of the DC servomotor shown in table 1, let the desired bandwidth of the current loop and velocity loop be 1 kHz and 100 Hz, respectively. The controller is obtained as $K_p = 12.747$, $K_i = 6252.5$, and $K_v = 16.721$ with the resulting bandwidths of the current loop and velocity loop are 99.797Hz and 997.63Hz, respectively.

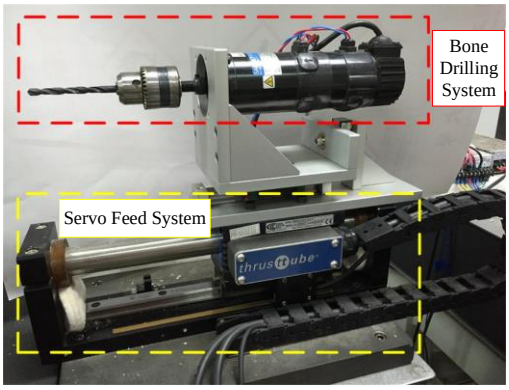

Figure 1. Experimental bone drilling system.

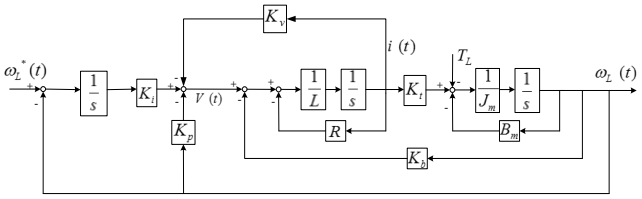

Figure 2. Structure of PID speed controller in DC drilling motor.

Table 1. Parameters of DC drilling motor

Parameters	Value
Resistance R	7.155 (Ω)
Inductance L	0.0038 (H)
Moment inertia J_m	5.77×10^{-5} ($kg\cdot m^2$)
Damping coefficient B_m	0.00055 ($N\cdot m\cdot s/rad$)
Back EMF constant K_e	0.21 ($V\cdot s/rad$)
Torque constant K_t	0.21 ($N\cdot m/A$)

3. Proposed breakthrough detection method

3.1. Chain scattering description

The CSD of a two-port network originated from the conventional electrical circuit theory [5]. The CSD developed in a network circuit provides a straightforward interconnection in a cascaded way. Thus, many known results that have been developed for a two-port network can then be used in control system analysis and synthesis. Due to its benefits of describing a linear system, the CSD was extended to analyze the characteristics of the proposed bone drilling system.

The bone drilling system applied in this paper is driven by a DC drilling motor. Consider the block diagram of a DC motor shown in figure 3, where Z_m denotes the equivalent mechanical impedance of loading.

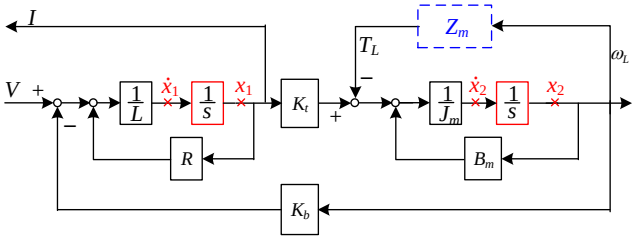

Figure 3. Block diagram of DC motor.

Let V (voltage reference) and T_L (load) be input variables, and I (motor current) and ω_L (motor angular velocity) be the outputs. A (2x2) LFT (linear fractional transformation) representation [5] of figure 3 is depicted in figure 4, as

$$\begin{bmatrix} I \\ \omega_L \end{bmatrix} = P(s)\begin{bmatrix} V \\ T_L \end{bmatrix} = \begin{bmatrix} P_{11}(s) & P_{12}(s) \\ P_{21}(s) & P_{22}(s) \end{bmatrix}\begin{bmatrix} V \\ T_L \end{bmatrix}, \tag{1}$$

where

$$P(s) = \begin{bmatrix} \dfrac{J_m s + B_m}{LJ_m s^2 + (LB_m + J_m R)s + (RB_m + K_b K_t)} & \dfrac{K_b}{LJ_m s^2 + (LB_m + J_m R)s + (RB_m + K_b K_t)} \\ \dfrac{K_t}{LJ_m s^2 + (LB_m + J_m R)s + (RB_m + K_b K_t)} & \dfrac{-(R + Ls)}{LJ_m s^2 + (LB_m + J_m R)s + (RB_m + K_b K_t)} \end{bmatrix}.$$

Through the reconstruction of the relationship between input and output in LFT form, the CSD of figure 5 with the "input" variables T_L, ω and the "outputs" I, V, can be derived from equation (1), as

$$\begin{aligned} \begin{bmatrix} I \\ V \end{bmatrix} &= \begin{bmatrix} P_{12}(s) - P_{11}(s)P_{21}^{-1}(s)P_{22}(s) & P_{11}(s)P_{21}^{-1}(s) \\ -P_{21}^{-1}(s)P_{22}(s) & P_{21}^{-1}(s) \end{bmatrix}\begin{bmatrix} T_L \\ \omega_L \end{bmatrix} \\ &= \begin{bmatrix} G_{11}(s) & G_{12}(s) \\ G_{21}(s) & G_{22}(s) \end{bmatrix}\begin{bmatrix} T_L \\ \omega_L \end{bmatrix} = G(s)\begin{bmatrix} T_L \\ \omega_L \end{bmatrix} \\ &= \begin{bmatrix} \dfrac{1}{K_t} & \dfrac{J_m s + B_m}{K_t} \\ \dfrac{R + Ls}{K_t} & \dfrac{LJ_m s^2 + (LB_m + J_m R)s + (RB_m + K_b K_t)}{K_t} \end{bmatrix}\begin{bmatrix} T_L \\ \omega_L \end{bmatrix} \end{aligned}, \tag{2}$$

where G is a so-called transduction matrix [9].

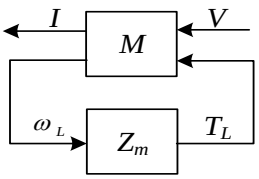

Figure 4. LFT form of DC motor.

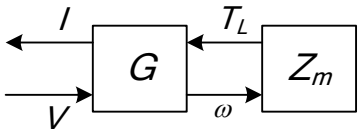

Figure 5. Two-port chain description matrix of a DC motor.

Thus, for any equivalent mechanical impedance of loading $Z_m(s)$, the equivalent electrical impedance of the motor, denoted by $Z_e(s)$, is given by

$$Z_e(s)=\frac{V}{I}=\frac{G_{21}(s)T_L+G_{22}(s)\omega_L}{G_{11}(s)T_L+G_{12}(s)\omega_L}=\frac{G_{21}(s)Z_m(s)+G_{22}(s)}{G_{11}(s)Z_m(s)+G_{12}(s)} \tag{3}$$

Reversely, if the electrical impedance $Z_e(s)$ is measured via V and I at the input-port of figure 5, then the equivalent impedance of mechanical loading at the output-port can be found as

$$Z_m(s)=\frac{-G_{12}(s)Z_e(s)+G_{22}(s)}{G_{11}(s)Z_e(s)-G_{21}(s)} \tag{4}$$

However, equation (4) is impracticable due to an improper transfer function as depicted in equation (2) [10]. In fact, (2) can be realized under a single frequency condition in practical application [9][11]. For instance, under the condition of 10Hz, i.e. s=jω=j10, the transduction matrix of equation (2) becomes

$$G(j10)=\begin{bmatrix} \frac{1}{K_t} & \frac{B_m}{K_t}+j\frac{20\pi J_m}{K_t} \\ \frac{R}{K_t}+j\frac{20\pi L}{K_t} & \frac{(RB_m+K_bK_t)-20\pi LJ_m}{K_t}+j\frac{(LB_m+J_mR)20\pi}{K_t} \end{bmatrix}. \tag{5}$$

Then, the 10Hz equivalent mechanical impedance of the load can be derived by equations (4) and (5) for the evaluation and determination of breakthrough. In the next subsection, the signal processing method, HHT, is adopted to evaluate the required characteristic component of the measured electrical signal for detecting the breakthrough of bone.

3.2. Signal processing

The Fast Fourier Transform (FFT) has been widely utilized in many signal processing applications; however, FFT is not capable of analyzing non-stationary signals, which might lead to inaccurate results, such as side lope and harmonics [12]. Hence, the HHT, an advanced time-frequency signal processing technique that is capable of analyzing non-stationary signals, real-time measurement and preservation of the characteristics of the varying frequency, is applied to analyze the measured electrical signal during the bone drilling process.

Given a tested signal $x(t)$, the EMD (Empirical mode decomposition) [6], a self-adaptive decomposition process for non-stationary and nonlinear signals can be described as

$$x(t)=\sum_{i}^{N} IMF_i(t)+r(t) \tag{6}$$

where N denotes IMF (Intrinsic mode functions) [6] modes and r(t) the residue. The IMFs are simple oscillatory functions with varying amplitudes and frequencies, which are defined to satisfy the following conditions [6]:

1. The number of extrema and the number of zero-crossing must either be equal or differ at most by one.
2. At any point, the mean value of the two envelopes defined by the local maxima and local minima is zero.

In practice, the procedure of EMD is as follows: firstly, identify all the local maxima (minima) and obtain the upper (lower) envelope by connecting all the local maxima (minima) with a cubic spline; secondly, obtain the candidate IMF by subtracting the data from the local mean of the two envelopes;

finally, check if the candidate IMF satisfies the definition of IMF; if not, repeat Steps 1 and 2 until the candidate IMF satisfies the definition of IMF.

A major drawback of the EMD is frequent occurrence of mode mixing. Mode mixing results from signal intermittency, which is defined as a signal of a similar scale residing in different IMF components [13]. Such a drawback makes the IMF lack physical meaning and causes serious aliasing in the time-frequency distribution. To alleviate this problem, EEMD (Ensemble empirical mode decomposition) [13], a major improvement on the EMD method, is applied in this paper.

The EEMD starts by adding white noise $w_m(t)$ into an intermittent tested signal $x(t)$ and converting it into a new continuous tested signal $x_m(t)$. Then, decomposing the tested signal $x_m(t)$ by EMD, the mode mixing can be eliminated due to that the white noise $w_m(t)$ distributes the whole time-frequency space uniformly. However, white noise will remain in each IMF. White noise has a unique property that allows it to cancel itself out; hence, a time-space ensemble mean is applied here. Therefore, the tested signal is decomposed repeatedly by adding in different white noises, and the ensemble means of the corresponding IMFs are acquired as the final IMFs. After the IMFs from EEMD are obtained, the instantaneous amplitude and frequency can be computed by applying HT to each IMF [6] as

$$\hat{F}_i(t) = HT\{F_i(t)\} = \frac{1}{\pi} PV \int_{-\infty}^{\infty} \frac{F_i(\tau)}{t-\tau} d\tau \tag{7}$$

in which the PV indicates the Cauchy principal value [14]. With the Hilbert transform $\hat{F}_i(t)$ of the function $F_i(t)$, the analytic function is

$$z(t) = F_i(t) + j\hat{F}_i(t) = a_i(t)e^{j\theta_i(t)} = a_i(t)e^{j2\pi\int f_i(t)dt} \tag{8}$$

where $a_i(t) = \sqrt{F_i^2(t) + \hat{F}_i^2(t)}$ denotes the instantaneous IMF amplitude, $\theta_i(t) = \tan^{-1}\frac{\hat{F}_i(t)}{F_i(t)}$ the instantaneous phase function, and $f_i(t) = \frac{1}{2\pi}\frac{d\theta_i(t)}{dt}$ the instantaneous IMF frequency.

3.3. Proposed breakthrough detection method

Generally speaking, the medullary cavity in human bone, which is filled with soft yellow marrow, is surrounded by dense strong cortical bone as illustrated in figure 6 [2]. The drill bit is performed on dense strong cortical bone along the soft yellow marrow during bone drilling surgery. Thus, the breakthrough of bone during bone drilling surgery can be detected by monitoring the equivalent mechanical impedance of bone.

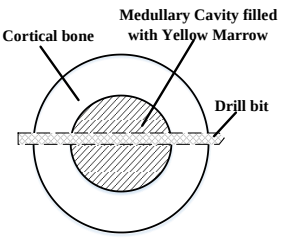

Figure 6. Cross-section of human bone [2].

As mentioned in the previous subsection, the equivalent mechanical impedance of bone can be determined from equation (4) and DC (0Hz) transduction matrix due to the DC drilling motor. However, the bone has inhomogeneous organic nature. It is hard to detect the breakthrough point precisely by monitoring the equivalent mechanical impedance only in a single frequency. Therefore, a

small amplitude sinusoidal signal in the specific frequency is injected into the reference velocity command $\omega_L^*(t)$ shown in figure 2 as

$$\omega_{L\_new}^*(t) = \omega_L^*(t) + a\sin(2\pi ft) \tag{9}$$

where a is a small constant value usually set as 1~2% of $|\omega_L^*(t)|$ to maintain the characteristic of the bone drilling system; f denotes the specific frequency. Consequently, the characteristics of specific frequencies become existent in the electrical signal (voltage and current) of the bone drilling system. In accordance with HHT, the measured electrical signals are analyzed for obtaining the DC signal and 10Hz specific frequency sinusoidal signal. Then, the equivalent mechanical impedances can be calculated via a single-frequency transduction matrix and provided for breakthrough detection.

4. Experiment results

The porcine bone demonstrates a good likeness with human bone [15]; hence, the proposed breakthrough detection method is validated by the experiment results of drilling porcine bone in this paper. The prototype of the experimental bone drilling system is shown in figure 1.

According to equation (9), a 10Hz sinusoidal signal is injected into the reference velocity command $\omega_L^*(t)$ after 1 sec as depicted in figure 7, where the amplitude a is 2% of $|\omega_L^*(t)|$. Therefore, the characteristic of a specific frequency becomes existent in the corresponding voltage *V(t)* and current *i(t)* as shown in figures 8 and 9. Moreover, the corresponding voltage *V(t)* and current *i(t)* are extracted and computed by applying the HHT as shown in figures 10 and 11; note that only IMF 5 and the residue are depicted here for brevity. Then, IMF 5 and the residue of the voltage *V(t)* and current *i(t)*, respectively, are implemented for equation (2) to compute the equivalent mechanical impedances at the condition of 10Hz and DC.

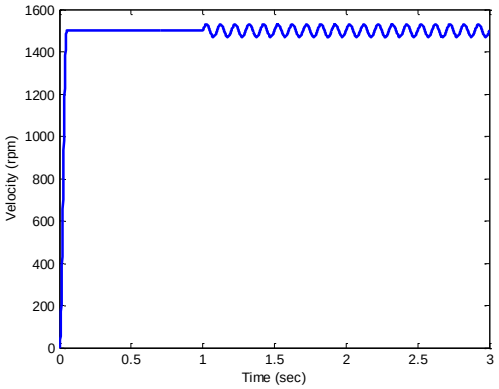

Figure 7. Reference velocity command injected with 10Hz sinusoidal signal.

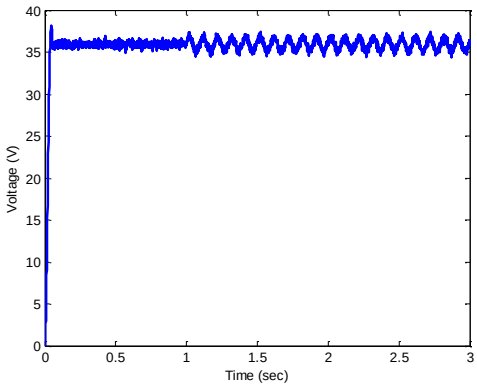

Figure 8. Driven voltage *V(t)* of bone drilling system.

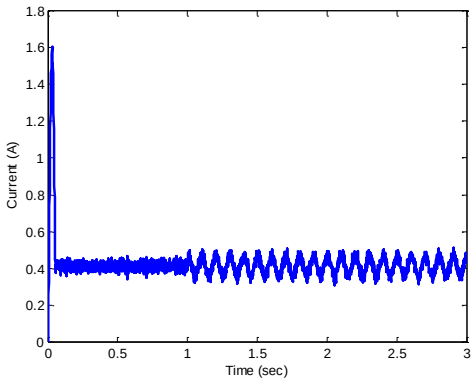

Figure 9. Measured current *i(t)* from bone drill system.

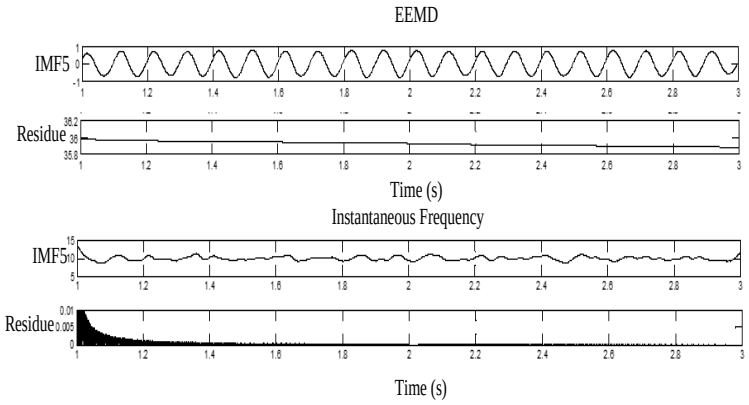

Figure 10. IMFs of driven voltage *V(t)* and corresponding instantaneous frequency.

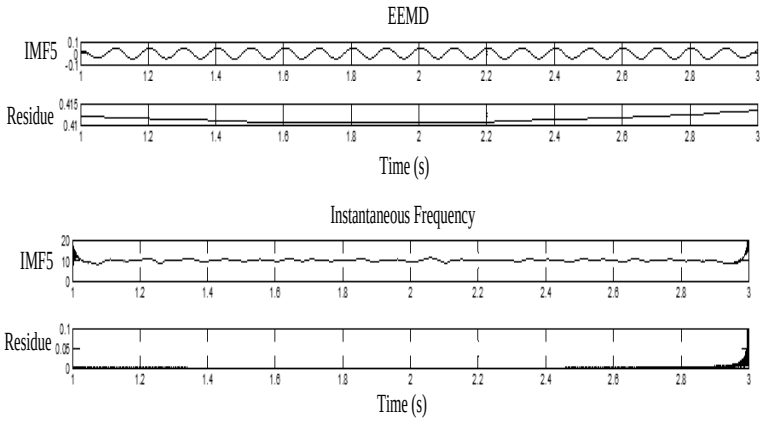

Figure 11. IMFs of measured current *i(t)* and corresponding instantaneous frequency.

Through monitoring the 10Hz and DC equivalent mechanical impedance, respectively, during the bone drilling process, the experiment results are illustrated in figure 12. From figure 12 (a), the DC equivalent mechanical impedance rises rapidly after 10 seconds, which indicates that the drill bit is in contact with bone. Afterward, the DC equivalent mechanical impedance dramatically decreases at 24 seconds and 65 seconds, which means that the bone drilling system penetrates the layers of the bone, respectively. The result of the specified frequency signal (10Hz) as shown in figure 12 (b) is similar to

figure 12 (a). Therefore, the moment of bone breakthrough is detected when second peak occurs in both DC and 10Hz equivalent mechanical impedance.

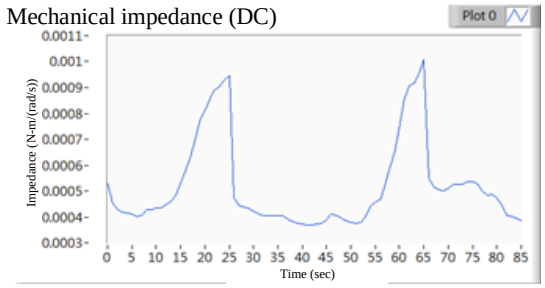

(a) DC equivalent mechanical impedance

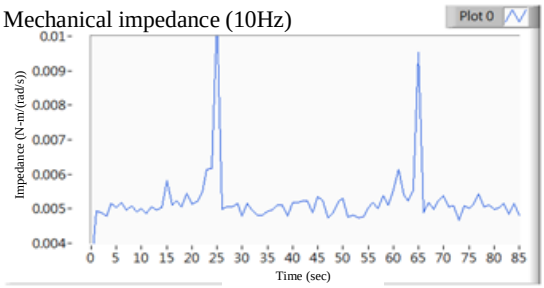

(b)10Hz equivalent mechanical impedance

Figure 12. Experiment results of monitoring equivalent mechanical impedance of bone at DC and 10Hz.

5. Conclusions

This paper has proposed a new approach for evaluating the equivalent mechanical impedance of the mechanical load of a DC motor without applying conventionally mechanical sensors. The proposed method employs the electrical signal of a DC motor to compute equivalent mechanical impedance based on Chain Scattering Description and Hilbert Huang Transform method. The proposed method was applied to the bone drilling system to detect the moment of bone breakthrough. The idea is to monitor the mechanical impedance of bone, which can establish the mechanism of breakthrough detection. The experimental results demonstrate that the proposed method can accurately evaluate the moment of bone breakthrough.

6. Acknowledgments

This work was supported by Ministry of Science and Technology of Taiwan, under project MOST 105-2218-E-006-008. The authors are grateful to Mr. Ming-Wei Shen, who contributed to pre-research of this study.

7. References

[1] Allotta B, Belmonte F, Bosio L and Dario P 1996 Study on a Mechatronic Tool for Drilling in the Osteosynthesis of Long Bones: Tool/Bone Interaction, Modeling and Experiments *Mechatronics* **6** 447-459.

[2] Ong F R and Bouazza-Marouf K 1998 Drilling of Bone: A Robust Automatic Method for the Detection of Drill Bit Break=Through *Proceedings of the Institution of Mechanical Engineerings, Part H: Journal of Engineering in Medicine* **212** 209-221.

[3] Colla V and Allotta B 1998 Wavelet-Based Control of Penetration in a Mechatronic Drill for Orthopaedic Surgery *IEEE International Conference on Robotics and Automation* **1** 711-716.

[4] Lee W Y, Shih C L and Lee S T Force Control and Breakthrough Detection of a Bone-Drilling System *IEEE/ASME Transactions on Mechatronics* **9** 20-29.

[5] Tsai M C and Gu D W 2014 *Robust and Optimal Control: A Two-Port Framework Approach* London: Springer-Verlag.

[6] Huang N E and Shen S S P 2014 Hilbert-Huang Transform and Its Applications *Interdisciplinary Mathematical Sciences* **16.**

[7] Ellis G 1991 *Control System Design Guide: Using your Computer to Develop and Diagnose Feedback Controllers* San Diego: Academic Press.

[8] Eriksson R A and Albrektsson T 1984 The Effect of Heat on Bone Regeneration: An Experimental Study in the Rabbit Using the Bone Growth Chamber *Journal of Oral & Maxillofacial Surgery* **42** 70.-711.

[9] Ling S F and Xie Y 2001 Detecting Mechanical Impedance of Structure Using the Sensing Capability of a Piezoceramic Inertial Actuator *Sensors and Actuators A* **93** 243-249.

[10] Sung S W, Lee J and Lee I B 2009 *Process Identification and PID Control* Wiley-IEEE Press.

[11] Liang C, Sun F and Rogers C 1996 A Electro-Mechanical Impedance Modeling of Active Material Systems *Smart Mater. Struct.* **5** 171-186.

[12] Rai V K and Mohanty A R 2005 Condition monitoring techniques for rolling element bearings: an overview *in Proceedings of National Conference on Role of NDE in Modern main Tenance Management* 8-18.

[13] Wu Z and Huang N E 2009 Ensemble empirical mode decomposition: a noise assisted data analysis method *Advances in Adaptive Data Analysis* **01** 1-41.

[14] Paget D F and Elliott D 1972 An algorithm for the numerical evaluation of certain Cauchy principal value integrals *Numerische Mathematik* **19** 373-385.

[15] Pearce A I, Richards R G, Milz S, Schneider E and Pearce S G 2007 Animal models for implant biomaterial research in bone: a review *European Cell and Materials* **13** 1-10.